Mathematical Sciences Letters
An International Journal

http://dx.doi.org/10.18576/msl/050101

Mechanisms of Different Nanoclusters in Nanobased Fluids with Natural Convection and Variable surface

M. Hassan[1], *R. Ellahi*[1,2,*] *and Ahmad Zeeshan*[1]

[1] Department of Mathematics & Statistics, IIUI, Islamabad, Pakistan.
[2] Department of Mechanical Engineering, University of California Riverside, USA.

Received: 8 Feb. 2015, Revised: 15 Oct. 2015, Accepted: 28 Oct. 2015
Published online: 1 Jan. 2016

Abstract: In this letter, the natural convection boundary layer flow with variable surface heat flux on nanofluids is investigated. Different nanoclusters containing different nano based fluids are taken into account. Analytic solutions are first obtained and then the role of sundry parameters such as heat flux gradient parameter, skin-friction, heat transfer coefficient and coefficient of nanofluid on velocity and temperature profiles are demonstrated through graphs and tables. Convergence of presenting series solutions has been conferred by means of error norm in their respective admissible range.

Keywords: Natural convection, variable surface heat flux, nanoclusters, nanofluid, analytical solutions.

1 Introduction

The problems concerning the flow of nanofluids have become more important nowadays. These fluids are widely encountered in the study of nanoparticles, nanofibers, nanotubes, nanowires, nanorods, nanosheet, or droplets etc. Nanofluids appear to have the potential to significantly increase the heat transfer rates in mechanical and electromechanical systems. Nanofluids are also found to possess enhanced thermophysical properties like thermal diffusivity, thermal conductivity, viscosity and convective heat transfer coefficients compared to those of base fluids like water and oil. It has demonstrated great potential applications in several other fields [1,2,3,4,5,6,7,8,9].

Moreover, noteworthy research efforts have been devoted to exploring the thermal transport characteristics of colloidal suspensions of nano-sized solid particles. Some recent studies having the related works on the topic can be mentioned by the efforts [10,11,12] Hong et al. [13] observed that the reduction of thermal conductivity of nanofluids is directly related to cluster of nanoparticles. In this study it has also mentioned that the thermal conductivity of Fe nanofluids increases nonlinearly by increasing the volume fraction of nanoparticles. The nonlinearity is attributed to the rapid clustering of nanoparticles in condensed nanofluids. The Fe nanofluids exposed a more rapid increase in thermal conductivity as compared to Cu nanofluids when the volume fraction of nanoparticles increased. They claim that the variations of cluster size and thermal conductivity both are functions of time. They also found that the thermal conductivity of nanofluids is closely related to the clustering of nanoparticles. With all said points in mind, we intend to strengthen our efforts to understand the problems having the more complicated nature. This is particularly in the modeling of different nanoclusters containing various nano-based fluids. To the best of authors' knowledge no study is still accorded in available literature on the said topic.

Motivated by these facts, the present work has been undertaken to analyze the fully developed flow of an incompressible nanofluid with different nanoparticle clustering containing free convection flow from a vertical circular cone with variable surface heat flux. To drive the solutions of nonlinear coupled equations, homotopy analysis method [14] has been used. Graphs for different flow parameters of interest are sketched and analyzed.

2 Mathematical formulation

We consider two dimensional free convection flows past a vertical circular cone with variable surface heat flux

* Corresponding author e-mail: rellahi@engr.ucr.edu

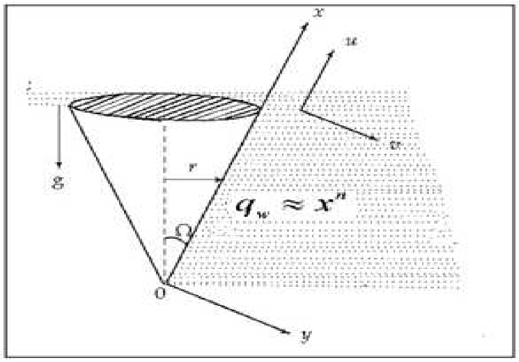

Fig. 1: Geometry of the problem.

having semi angle ˇ3a9. The flow configurations along with coordinate system are displayed in Fig. 1.

Let us consider the water and ethylene glycol based nanofluid comprising body centered cubic clusters, simple cubic clusters, face centered cubic clusters of TiO_2 and SiO_2 having nanoparticles of 10 nm diameter. The governing equations along with corresponding boundary conditions are

$$\frac{\partial}{\partial x}(ru)+\frac{\partial}{\partial y}(rv)=0, \tag{1}$$

$$\rho_{nf}\left(u\frac{\partial u}{\partial x}+v\frac{\partial u}{\partial y}\right)=\mu_{nf}\frac{\partial^2 u}{\partial y^2}+(\rho\beta)_{nf}\,g\,(T-T_\infty)Cos\Omega, \tag{2}$$

$$u\frac{\partial T}{\partial x}+v\frac{\partial T}{\partial y}=\alpha_{nf}\frac{\partial^2 T}{\partial y^2}. \tag{3}$$

$$u=0,\quad v=0,\quad q=-k_{nf}\frac{\partial T}{\partial y}\ \text{ at }\ y=0, \tag{4}$$

$$u=0,\quad T=T_\infty,\ at\ y\to\infty, \tag{5}$$

where $r=x\ Sin\Omega$ is a thin boundary layer, u is velocity component in $x-$direction, v is velocity component in $y-$direction, g is gravitational acceleration, ρ_{nf} is effective density, $(\rho C_p)_{nf}$ is capacitance, β_{nf} is thermal expansion coefficient and α_{nf} is thermal diffusibility of nanofluid. Mathematically it can be written as

$$\rho_{nf}=(1-\phi)\rho_f+\phi\rho_s, \tag{6}$$

$$(\rho C_p)_{nf}=(1-\phi)(\rho C_p)_f+\phi(\rho C_p)_s \tag{7}$$

$$\beta_{nf}=\frac{(1-\phi)(\rho\beta)_f+\phi(\rho\beta)_s}{\rho_{nf}}, \tag{8}$$

$$\alpha_{nf}=\frac{k_{nf}}{(\rho C_p)_{nf}}. \tag{9}$$

Table 1: Shapes of simple cubic clusters, body centered cubic clusters, face-centered cubic clusters for and nanofluids.

Nanoclusters	Simple cubic	Body centered	Face centered
φ_c	0.4875	0.6056	0.6891
$\gamma_p\,(nm)$	26.2255	26.2255	28.1617

Here, ϕ is solid volume fraction, β_f is thermal expansion coefficient of base fluid, β_s is thermal expansion coefficient of nanoparticle, ρ_f is density of basic fluid and ρ_s is density of nanoparticle. The thermal conductive models for nanofluid containing clusters [15] is given by

$$k_{nf}=\frac{k_s+2k_f-2\varphi\varphi_c\,(k_f-k_s)}{k_s+2k_f+\varphi\varphi_c\,(k_f-k_s)}k_f+2.1d_f\frac{\left[2+\left(\frac{K_bT\rho_fC_p}{\pi\mu_{nf}\,k_f\,\gamma_p}\right)\right]}{\gamma_p}k_f. \tag{10}$$

The viscosity model [16] for nanofluid is

$$\mu_{nf}=\frac{\mu_f}{1-34.87\left(\frac{d_p}{d_f}\right)^{-.3}\phi^{1.03}}, \tag{11}$$

where d_f is diameter of base fluid molecule, d_p is diameter of particle, K_b is Boltzmann constant, φ_c is volumetric ratio, $\varphi=\frac{\phi/\varphi_c}{1-\phi/\varphi_c+\phi}$ is volume fraction of nanoclusters and γ_p is mean diameter of nanoclusters. The values of φ_c and γ_p for shape of simple cubic clusters, body centered cubic clusters, face-centered cubic clusters are given in table 1. The shapes of these nanoclusters are shown in Fig. 2.

The volume fraction and the mean diameter nanoclusters for TiO_2 and SiO_2 nanofluid is given by

Using the stream function $\psi(x,y)$, the continuity equation is satisfied by the following expressions

$$u=\frac{1}{r}\frac{\partial\psi}{\partial y},\quad v=-\frac{1}{r}\frac{\partial\psi}{\partial x}. \tag{12}$$

In view of the following transformation [17]

$$\left.\begin{array}{l}\eta=\frac{y}{x}G_{rx}^{\frac{1}{5}},\quad \psi=v_frG_{rx}^{\frac{1}{5}}f(\eta),\\ T-T_\infty=\frac{q_wx}{k_f}G_{rx}^{-\frac{1}{5}}\theta(\eta),\ q_w=x^n\end{array}\right\}, \tag{13}$$

Eqs. (1) to (3) along with the boundary conditions (4) and (5) in non-dimensional form can be written as

$$\frac{\rho_{nf}}{\rho_f}\left[\left(\frac{2n+3}{5}\right)f'^2-\left(\frac{n+9}{5}\right)ff''\right]=\frac{\mu_{nf}}{\mu_f}f'''+Cos\Omega\frac{(\rho\beta)_{nf}}{(\rho\beta)_f}\theta, \tag{14}$$

$$P_r\frac{(\rho C_p)_{nf}}{(\rho C_p)_f}\left[\left(\frac{4n+1}{5}\right)\theta f'-\left(\frac{n+9}{5}\right)f\theta'\right]=\frac{k_{nf}}{k_f}\theta'' \tag{15}$$

$$f=0,\quad f'=0,\quad \theta'=-\frac{k_f}{k_{nf}}\quad \text{when}\quad \eta=0, \tag{16}$$

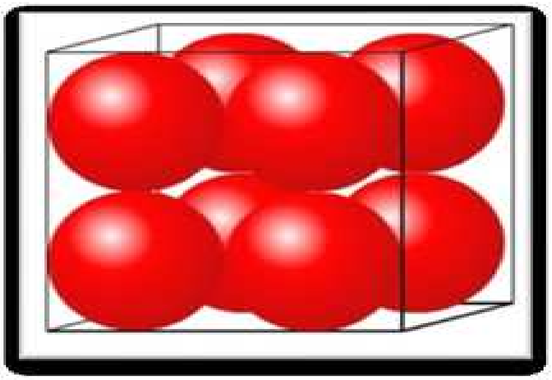

(a)

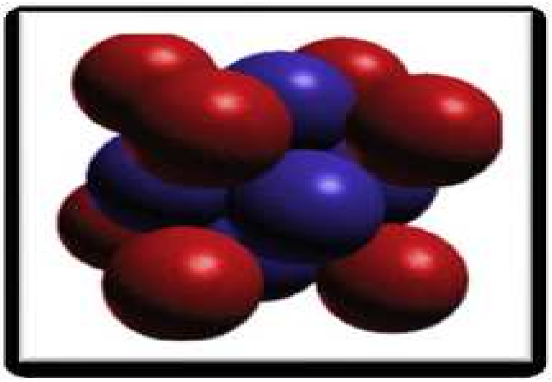

(b)

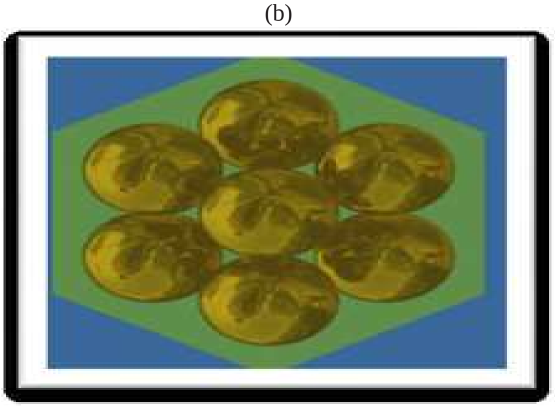

(c)

Fig. 2: (a) Simple cubic clusters, (b) Body centered cubic clusters (c) Face-centered cubic clusters.

$$f' = 0, \quad \theta = 0 \quad \text{when } \eta \longrightarrow \infty, \tag{17}$$

where $P_r = \nu_f/\alpha_f$ is Parental number and $G_{r_x} = g\beta_f q_w x^4/k_f \nu_f^2$ is Rayleigh number. The local Skin-friction coefficient C_{fx} and Nusselt number Nu_x are defined as

$$C_{fx} = \frac{2\tau_w}{\rho U^2} \quad \text{and} \quad Nu_x = -\frac{q_w x}{k_f (T_w - T_\infty)} \tag{18}$$

in which $\tau_w = \mu_{nf}\left(\frac{\partial u}{\partial y}\right)_{y=0}$ is shear stress, $q_w = -k_{nf}\left(\frac{\partial T}{\partial y}\right)_{y=0}$ is the rate of heat flux at surface and $U = \nu_f Gr_x^{2/5}/x$ is reference velocity. By using the transformation given in Eq. (13), the local Skin-friction coefficient and Nusselt number are obtained as

$$Gr_x^{1/5} C_{fx} = 2\left(\frac{\mu_{nf}}{\mu_f}\right) f''(0), \; Gr_x^{-1/5} Nu_x = \frac{1}{\theta(0)}. \tag{19}$$

3 Method of Solution

Our interest in this section is carried out the analytical solutions for the velocity and temperature distributions. In order to serve the said purpose the initial approximations of $f(\eta)$ and $\theta(\eta)$ are

$$f_0(\eta) = \frac{1}{2} + \frac{1}{2}e^{-2\eta} - e^{-\eta}, \qquad \theta_0(\eta) = \frac{k_f}{k_{nf}} e^{-\eta}. \tag{20}$$

By using differential mapping. we choose the following linear operators $\pounds_1$ and $\pounds_2$

$$\pounds_1(f) = \frac{d}{d\eta}\left(\frac{d^2 f}{d\eta^2} - f\right), \qquad \pounds_2(\theta) = \left(\frac{d^2}{d\eta^2} - 1\right)\theta. \tag{21}$$

We now construct the homotopy

$$\mathscr{H}_1[f(\eta,p)] = (1-p)\pounds_1[(f(\eta,p) - f_0(\eta)] - p\hbar_1 \mathscr{N}_1[f(\eta,p), \theta(\eta,p)], \tag{22}$$
$$\mathscr{H}_2[\theta(\eta,p)] = (1-p)\pounds_2[\theta(\eta,p) - \theta_0(\eta)] - p\hbar_2 N_2[f(\eta,p), \theta(\eta,p)], \tag{23}$$

where $\hbar_i (i = 1,2)$ is convergence parameter whereas embedding parameter $p \in [0,1]$. For zeroth order deformation problems, letting $\mathscr{H}_1[f(\eta,p)] = 0 = \mathscr{H}_2[\theta(\eta,p)]$, we get

$$(1-p)\pounds_1[f(\eta,p) - f_0(\eta)] = p\hbar_1 N_1[f(\eta,p), \theta(\eta,p)], \tag{24}$$

$$(1-p)\pounds_2[\theta(\eta,p) - \theta_0(\eta)] = p\hbar_2 N_2[f(\eta,p), \theta(\eta,p)], \tag{25}$$

$$f(\eta,p) = 0, \quad \frac{\partial f(\eta,p)}{\partial \eta} = 0, \quad \frac{\partial \theta(\eta,p)}{\partial \eta} = -\frac{k_f}{k_{nf}} \text{ at } \eta = 0, \tag{26}$$
$$f(\eta,p) = 0, \quad \theta(\eta,p) = 0 \quad \text{at} \quad \eta \to \infty. \tag{27}$$

The nonlinear operators N_1 and N_2 are

$$\mathscr{N}_1[f(\eta,p), \theta(\eta,p)] = \left(\frac{2n+3}{5}\right) f'^2(\eta,p) - \left(\frac{n+9}{5}\right) f(\eta,p) f''(\eta,p) \tag{28}$$
$$- \frac{\mu_{nf}}{\mu_f} f'''(\eta,p) + Cos\Omega \frac{(\rho\beta)_{nf}}{(\rho\beta)_f} \theta(\eta,p),$$

$$\mathscr{N}_2[f(\eta,p), \theta(\eta,p)] = P_r \frac{(\rho C_p)_{nf}}{(\rho C_p)_f} \left[\begin{array}{c} \left(\frac{4n+1}{5}\right)\theta(\eta,p) f'(\eta,p) - \\ \left(\frac{n+9}{5}\right) f(\eta,p)\theta'(\eta,p) \end{array} \right] - \frac{k_{nf}}{k_f}\theta''(\eta,p). \tag{29}$$

For $p = 0$

$$f(\eta,0) = f_0(\eta), \quad \theta(\eta,0) = \theta_0(\eta). \tag{31}$$

For $p = 1$

$$f(\eta,1) = f(\eta) \quad \theta(\eta,1) = \theta(\eta). \tag{32}$$

When p increases from 0 to 1, f and θ varies form initial approximations $f_0(\eta)$ and $\theta_0(\eta)$ to final solutions $f(\eta)$ and $\theta(\eta)$. By using Maclaurin's series, we obtain

$$f(\eta,p) = f_0(\eta) + \sum_{m=1}^{\infty} f_m(\eta)\, p^m, \tag{32}$$

$$\theta(\eta,p) = \theta_0(\eta) + \sum_{m=1}^{\infty} \theta_m(\eta)\, p^m, \tag{33}$$

where

$$\theta_m(\eta) = \frac{1}{m!}\frac{\partial\, \theta^m(\eta,p)}{\partial p^m}\bigg|_{p=0}, \quad f(\eta) = \frac{1}{m!}\frac{\partial\, f^m(\eta,p)}{\partial p^m}\bigg|_{p=0}. \tag{34}$$

Differentiating the zeroth-order deformation Eqs. (22) to (27) $m-$times with respect to the embedding parameter p, then dividing it by $m!$ and finally setting $p = 0$, we gain $mth-$order deformation equations [18] for $f_m(\eta)$ and $\theta_m(\eta)$ as follows

$$\pounds_1\left[f_m(\eta) - \chi_m f_{m-1}(\eta)\right] = \hbar_1 R1_m(\eta), \tag{35}$$

$$\pounds_2\left[\theta_m(\eta) - \chi_m \theta_{m-1}(\eta)\right] = \hbar_2 R2_m(\eta), \tag{36}$$

$$f_m(\eta,p) = 0, \quad \frac{\partial f_m(\eta,p)}{\partial\eta} = 0, \quad \frac{\partial\theta_m(\eta,p)}{\partial\eta} = 0 \text{ at } \eta = 0 \tag{37}$$

$$f_m(\eta,p) = 0, \quad \theta_m(\eta,p) = 0 \quad \text{at } \eta \to \infty, \tag{38}$$

where the recurrence relations are

$$R1_m(\eta) = \left(\frac{2n+3}{5}\right)\sum_{k=0}^{m} f'_k f'_{m-k} - \left(\frac{n+9}{5}\right)\sum_{k=0}^{m} f_k f''_{m-k} - \tag{39}$$

$$-\frac{\mu_{nf}}{\mu_f} f'''_m + Cos\Omega \frac{(\rho\beta)_{nf}}{(\rho\beta)_f}\theta_m,$$

$$R2_m(\eta) = P_r \frac{(\rho C_p)_{nf}}{(\rho C_p)_f}\left[\left(\frac{4n+1}{5}\right)\sum_{k=0}^{m}\theta_m f'_{m-k} - \left(\frac{n+9}{5}\right)\sum_{k=0}^{m} f_m \theta'_{m-k}\right] - \frac{k_{nf}}{k_f}\theta''_m, \tag{40}$$

$$\chi_m = \begin{cases} 0, & m \le 1, \\ 1, & m > 1. \end{cases} \tag{41}$$

The final solutions can be expressed as

$$f(\eta) = f_0(\eta) + \sum_{k=1}^{m} f_k(\eta), \tag{42}$$

$$\theta(\eta) = \theta_0(\eta) + \sum_{k=0}^{m} \theta_k(\eta). \tag{43}$$

4 Results and Discussion

The convergence region and rate of approximations given by [19] are strongly dependent upon the control parameters $\hbar_1$ and $\hbar_2$. The error norms for two successive approximations over $[0,1]$ by $15th$-order approximations are calculated by

$$E_f = \sqrt{\frac{1}{16}\sum_{i=0}^{15}\left(f_{15}(i/15)\right)^2} \tag{44}$$

$$E_\theta = \sqrt{\frac{1}{16}\sum_{i=0}^{15}\left(\theta_{15}(i/15)\right)^2}. \tag{45}$$

It is found that the errors for velocity and temperature are minimum at $\hbar_1 = -0.52$ and $\hbar_2 = -0.59$ respectively. These values lie in their respective admissible range.

To see the effects of emerging parameters of interest on flow quantities such as velocity, temperature and volume-fraction of nanoparticles Figs. 3 to 10 have been prepared for velocity, temperature distribution and table 2 is for sink fiction coefficient and Nusselt number of water based nanofluid containing nanoclusters of TiO_2 nanoparticles. In the entire analysis we also assumed air temperature $300K$ and $Pr = 0.71$. Figs. 3 and 4 show the behavior of nanoparticles fiction respectively on velocity and temperature profiles in the presence of simple cubic cluster, body centered cubic cluster and face centered cubic cluster when $n = 1$. These figures illustrate that when friction of particles is increased from 0.02 to 0.04, the velocity and temperature are decreasing and increasing functions respectively. In the velocity profile, maximum decrease is observed in simple cubic nanoclusters containing nanofluid and maximum increase is happening with face centered cubic cluster containing nanofluid. On the other hand, the maximum temperature of fluid is increased and decreased by face centered cubic and simple cubic nanoclusters nanofluid respectively. The Figs. 5 and 6 display the effects of nanoclusters on velocity and temperature by changing the based fluids. In the velocity and temperature profile, maximum increase is observed by face centered cubic cluster in water and ethylene glycol based nanofluid when $n = 1$ and $\phi = 0.04$. The Figs. 5 and 6 also show that when we choose ethylene glycol based nanofluid, the velocity and temperature of fluid are decreased for water based nanofluid in the presence of TiO_2 nanoclusters. Figs. 7 and 8 demonstrate the effects of nanoclusters on velocity and temperature by changing the nanoclusters of different nanoparticles. In the velocity and temperature profiles, maximum decrease is observed in simple cubic clusters of TiO_2 than SiO_2 metals for water based nanofluid when $n = 1$ and $\phi = 0.04$. These figures point out that velocity profile maximum reduces by TiO_2 nanoclusters and thermal profile maximum increases by TiO_2 nanoclusters. The Figs. 9 and 10 express the impact of different values of surface heat flux parameter (n) on velocity and

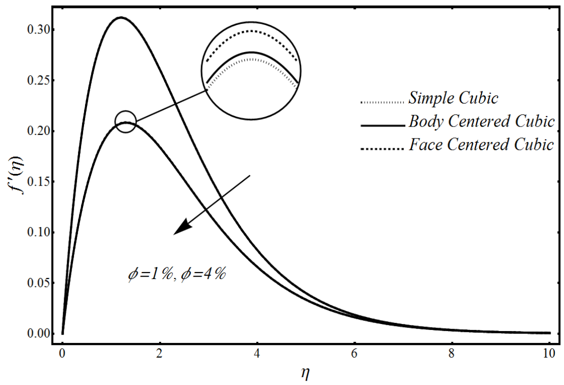

Fig. 3: Variation of volume friction on velocity profile in the presence of nanoclusters.

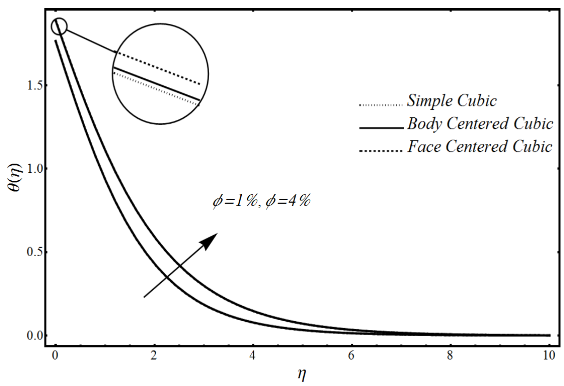

Fig. 4: Variation of volume friction on temperature profile in the presence of nanoclusters.

temperature structures when $\phi = 0.04$. It is observed that velocity and temperature are declined by an enhancement in value of n.

The table 2 demonstrates the results of skin-friction and heat transfer coefficient when $n = 1$ and $\phi = 0.04$. It is observed that with the increase of volume friction, the skin-friction coefficient decreases whereas the heat transfer coefficient is increasing for all types of TiO_2-nanoclusters containing water based nanofluid.

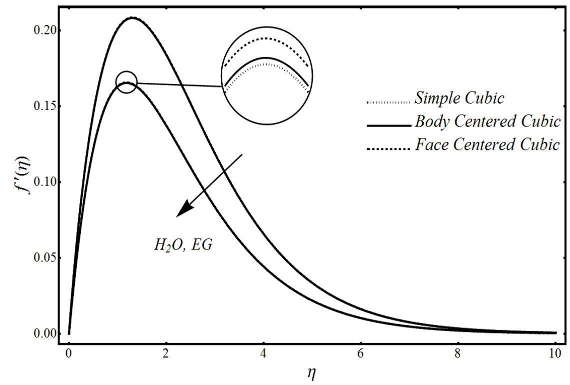

Fig. 5: Variation of different based fluids on velocity profile in the presence of nanoclusters.

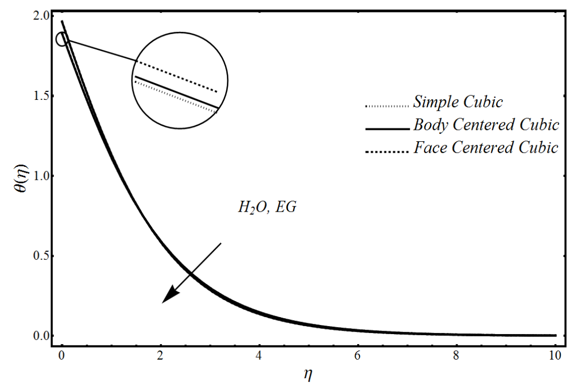

Fig. 6: Variation of different based fluids on velocity profile in the presence of nanoclusters.

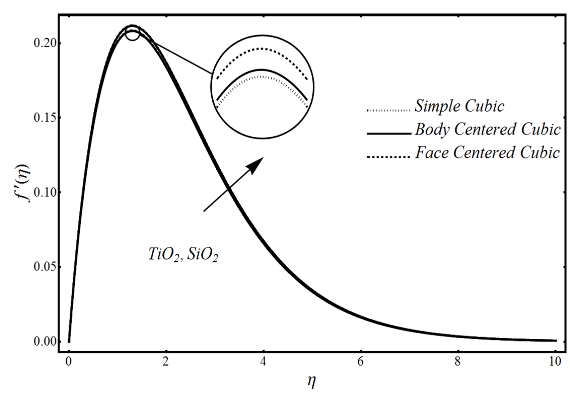

Fig. 7: ffects of clusters for different nanoparticles on velocity profile.

Table 2: Correlation of Skin-friction and heat transfer coefficient TiO_2-nanofluid

Clusters	ϕ	Simple cubic	Body centered cubic	Face centered cubic
$f''(0)$	0.02	0.834691	0.834767	0.835605
	0.04	0.794614	0.794893	0.795738
$1/\theta(0)$	0.02	0.723330	0.723189	0.721648
	0.04	0.732549	0.732282	0.730288

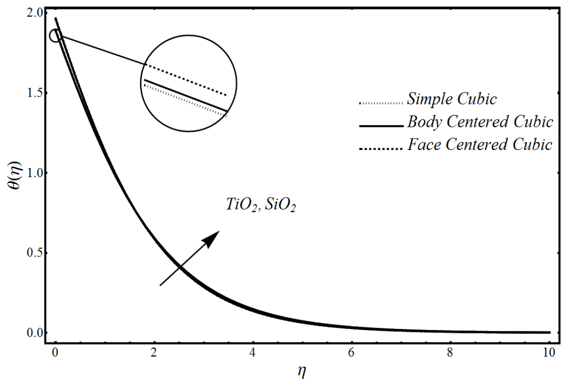

Fig. 8: Effects of clusters for different nanoparticles on temperature profile.

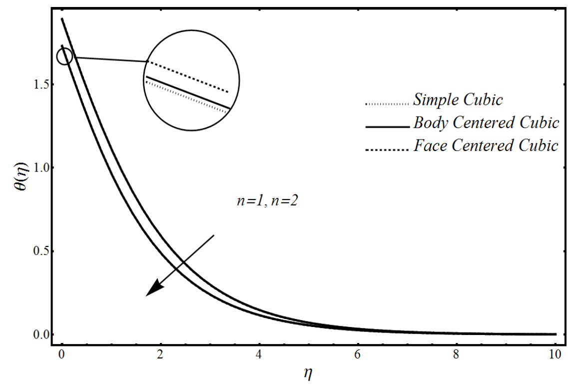

Fig. 10: Effects of flux gradient parameter on temperature profile in the presence of nanoclusters.

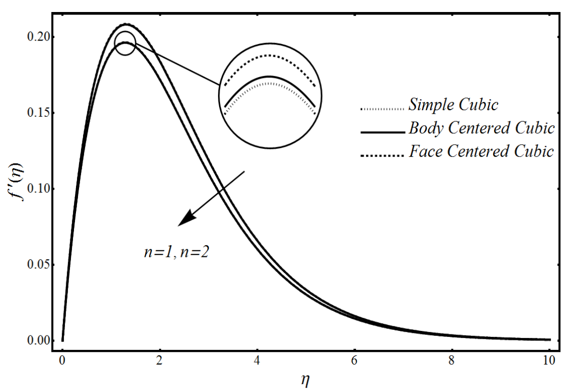

Fig. 9: Effects of flux gradient parameter on velocity profile in the presence of nanoclusters.

5 Conclusions

In this letter, the different nanoclusters behavior on velocity and temperature of nanofluid have been analyzed by changing based fluid and nanoparticles. It is found that face centered cubic clusters have the same behavior for velocity and temperature profiles even for different based fluid and nanoparticles. Face centered cubic clusters give the maximum velocity and temperature when compared with other types of clusters. It is seen that the velocity of fluid is decreasing with the effects of particle volume friction and flux gradient parameters. On the other hand, temperature increases for particle volume friction but decreases for surface heat flux parameter. Tabulated results are presented to see the effects of particle volume friction on Skin-friction and heat transfer coefficient. It is observed that the Skin-friction and heat transfer coefficient are respectively decreasing and increasing when value of volume friction is increased for all nanoclusters.

References

[1] S. Nadeem, Aziz Ur Rehman, Rashid Mehmood and M. Adil Sadiq, Partial Slip Effects on a Rotating Flow of Two Phase Nano Fluid Over a Stretching Surface, Current Nanoscience, 10(6), (2014), 846-854.
[2] Noreen Sher Akbar, S. Nadeem, Changhoon Lee and Z. H. Khan, Numerical simulation of nanoparticle fraction for the peristaltic flow of a six constant Jeffrey's fluid model, Current Nano Sciences, 9(2013) 798 - 803.
[3] Noreen Sher Akbar, MHD peristaltic flow of a nanofluid with Newtonian heating, Current Nano Sciences, 16(6), 2014.
[4] Duangthongsuk W., Dalkilic A. S., Wongwises S. Convective heat transfer of Al2O3-water nanofluids in a microchannel heat sink, Current Nanoscience, 8(3) (2012), 317 – 322.
[5] R. Ellahi, A. Zeeshan and M. Hassan, Shape effects of nanosize particles in Cu-H2̌0820 nanofluid on entropy generation, International Journal of Heat and Mass Transfer, 81 (2015), 449–456.
[6] N. Bachok, A. Ishak, I. Pop, Boundary-layer flow of nanofluids over a moving surface in a flowing fluid,

International Journal of Thermal Sciences, 49 (2010), 1663-1668.
[7] N. A. Yacob, A. Ishak, I. Pop, Falkner-Skan problem for a static or moving wedge in nanofluids, International Journal of Thermal Sciences, 50 (2011), 133-139.
[8] R. Ellahi, The effects of MHD and temperature dependent viscosity on the flow of non-Newtonian nanofluid in a pipe: analytical solutions, Applied Mathematical Modelling, 37(3), (2013), 1451-1457.
[9] M. Sheikholeslami, R. Ellahi, Mohsen Hassan and S. Soleimani,. A study of natural convection heat transfer in a nanofluid filled enclosure with elliptic inner cylinder, International Journal for Numerical Methods for Heat and Fluid Flow, 24 (8), (2014), 1906-1927.
[10] Keblinksi, P. S. R. Phillpot, S. U. S. Choi, J. A. Eastman, Mechanisms of heat flow in suspensions of nano-sized particles (nanofluids), International Journal of Heat and Mass Transfer, 45 (2002) 855-863.
[11] B. X. Wang, W. Y. Sheng, X. F. Peng, A novel statistical clustering mode for predicting thermal conductivity of nanofluid, International journal of Thermo physics, 30 (2009) 1992-1998.
[12] N. R. Kathikeyan, J. Philip, B. Raj, Effect of clustering on the therma conductivity of nanofluids, Materials Chemistry and Physics, 109 (2008) 50-55.
[13] K. S Hong, T. K. Hong, H. S. Yang, Thermal conductivity of Fe nanofluids depending on the cluster size of nanoparticles, Applied Physics Letters, 88, (2006) 0319011-0319013.
[14] A. Zeeshan and R. Ellahi, Series solutions of nonlinear partial differential equations with slip boundary conditions for non-Newtonian MHD fluid in porous space, Journal of Applied Mathematics & Information Sciences, 7 (1) (2013) 253-261.
[15] A. N. Chinnaraj, Theses: Thermal conductive enhancement in nanofluid-Mathematical Model, Southern Illinois University Carbondale, (2011).
[16] D, Kim, Y. Kwon, Y. Cho, C. Li, S. Cheong, Y. Hwang,J. Lee, D. Hong, S. Moon, Convective heat transfer characteristics of nanofluids under laminar and turbulent flow conditions, Current Applied Physics, 9 (2009) 119-123.
[17] E. M. A. Elbashbeshy, T. G. Emam, E. A. Sayed, Effect of pressure work and heat generation / absorption on free convection flow from a vertical circular cone with variable surface heat flux, World J. of Eng. & Physical Sci., 1 (2) (2013) 17-25.
[18] S. J. Liao, Beyond Perturbation: Introduction to Homotopy Analysis Method. Chapman & Hall. Boca Raton, 2003.
[19] S. J. Liao, An analytic approximate technique for free oscillations of positively damped systems with algebraically decaying amplitude. Int. J. Non-Linear Mech. 38 (2003) 1173-1183.

Mohsin Hassan Is doing his PhD under the supervision of R. Ellahi at IIUI, Pakistan. He obtained his MS from IIUI. His research work has been published in internationally refereed journals.

Rahmat Ellahi Is Chairperson of the Department at IIUI and received outstanding research awards such as Productive Scientist Award, Best Book Award, and Valued Reviewer Award by Elsevier. He is a Fulbright Fellow of University of California Riverside USA. He is also the recipient of best book award, Best University Teacher Award and highly cited paper award. He is editor of 07 international journals and review panels of more than 150 ISI impact factor journals. His work has been cited more than 2100 times. He has supervised several research students at MS and PHD level. He has carried out various sponsored research projects through governmental funding. He is an author of 06 books and actively involved in different academic bodies at national and international level.

Ahmad Zeeshan Did his PhD degree with distinction under the supervision of R. Ellahi and is working as assistant professor at IIUI Pakistan. His field of research is Fluid Mechanics and he has supervised few students at MS level. His research articles have been published in the journals of international repute.